

# Chemical Science

Accepted Manuscript



This is an *Accepted Manuscript*, which has been through the Royal Society of Chemistry peer review process and has been accepted for publication.

*Accepted Manuscripts* are published online shortly after acceptance, before technical editing, formatting and proof reading. Using this free service, authors can make their results available to the community, in citable form, before we publish the edited article. We will replace this *Accepted Manuscript* with the edited and formatted *Advance Article* as soon as it is available.

You can find more information about *Accepted Manuscripts* in the [Information for Authors](#).

Please note that technical editing may introduce minor changes to the text and/or graphics, which may alter content. The journal's standard [Terms & Conditions](#) and the [Ethical guidelines](#) still apply. In no event shall the Royal Society of Chemistry be held responsible for any errors or omissions in this *Accepted Manuscript* or any consequences arising from the use of any information it contains.

## ARTICLE

# Ultrafast photoinduced electron transfer in face-to-face charge-transfer $\pi$ -complexes of planar porphyrins and hexaazatriphenylene derivatives†

Cite this: DOI: 10.1039/x0xx00000x

Received 00th January 2012,  
Accepted 00th January 2012

DOI: 10.1039/x0xx00000x

www.rsc.org/

Toru Aoki,<sup>a</sup> Hayato Sakai,<sup>a</sup> Kei Ohkubo,<sup>b</sup> Tomo Sakanoue,<sup>c</sup> Taishi Takenobu,<sup>\*,c</sup> Shunichi Fukuzumi,<sup>\*,b</sup> and Taku Hasobe<sup>\*,a</sup>

Charge-transfer (CT)  $\pi$ -complexes are formed between planar porphyrins and 1,4,5,8,9,12-hexaazatriphenylene (HAT) derivatives with large formation constants (e.g.,  $10^4 \text{ M}^{-1}$ ), exhibiting broad CT absorption bands. The unusually large formation constants result from close face-to-face contact between two planar  $\pi$ -planes of porphyrins and HAT derivatives. The redox potentials of porphyrins and HAT derivatives measured by cyclic voltammetry indicate that porphyrins and HAT derivatives act as electron donors and acceptors, respectively. Formation of 1 : 1 CT complexes between porphyrins and HAT derivatives was examined by the UV-vis, fluorescence and  $^1\text{H}$  NMR measurements in nonpolar solvents. The occurrence of unprecedented ultrafast photoinduced electron transfer from the porphyrin unit to the HAT unit in the CT  $\pi$ -complex was observed by femtosecond laser flash photolysis measurements. Highly linear aggregate composed of a planar porphyrin and an HAT derivative was observed by transmission electron microscope (TEM) and atomic force microscope (AFM).

## Introduction

Extensive efforts have so far been devoted to construction of covalently linked electron donor-acceptor (D-A) ensembles to mimic efficient photoinduced electron-transfer processes in the photosynthetic reaction center, which is essential to realize artificial photosynthesis.<sup>1-9</sup> Non-covalent interactions have also been utilized to construct more sophisticated D-A ensembles with highly ordered nanoarchitectures.<sup>10-19</sup> The use of non-covalent interactions has great advantage over the step-by-step synthesis of many covalent bonds due to the self assembling features of supramolecules with non-covalent interactions. However, supramolecular D-A ensembles have disadvantage in terms of weak interactions between electron donors and acceptors, which have prohibited ultrafast photoinduced electron transfer via through space.<sup>10-19</sup>

In order to surmount such disadvantage of supramolecular D-A ensembles, the non-covalent interactions should be strengthened by close contact of two large planar  $\pi$ -planes of electron donors and acceptors. Porphyrins which have a large planar  $\pi$ -plane have been used as good electron donors as well as chromophores absorbing visible light in D-A ensembles (e.g., electrostatic host-guest assemblies with  $\text{C}_{60}$ ).<sup>2-5,14-20</sup> On the other hand, there are many examples of supramolecular assemblies of porphyrins, in which efficient energy transfer occurred.<sup>20-22</sup> Thus, porphyrins act as electron donors or energy

acceptors but not electron acceptors due to the low one-electron reduction potentials. Although a variety of supramolecular D-A ensembles have been reported so far, there has been no example of supramolecular D-A ensembles composed of porphyrins utilizing the simple close face-to-face contact for occurrence of ultrafast photoinduced electron transfer.

Disc-like polycyclic aromatic hydrocarbon (PAH) derivatives such as triphenylene (TPh) functionalized with alkyl groups, which self-assemble into supramolecular columnar structures with hexagonal and nematic phases because of the stacking  $\pi$ - $\pi$  interactions,<sup>23-26</sup> may be a good candidate for an electron acceptor to construct face-to-face complexes with planar porphyrins. In this context, 1,4,5,8,9,12-hexaazatriphenylene (HAT) derivatives have merited special attention, because these molecules possess the electron deficient pyrazine units, acting as good electron acceptors.<sup>27,28</sup> Moreover, hexaazatriphenylene hexacarbonitrile (HAT-CN) and hexaazatriphenylene-hexacarboxy triimide (HAT-TIm) have a quite low-lying energy of LUMO as compared to the pristine HAT because of introduction of strong electron withdrawing groups such as nitrile and imide groups. The reported lowest unoccupied molecular orbital (LUMO) level of HAT-CN (-4.4 eV)<sup>29</sup> and first reduction potential of HAT-TIm (-0.35 V vs SCE)<sup>30</sup> indicate the efficient electron accepting properties, which are even better than  $\text{C}_{60}$  (-0.44 V vs SCE).<sup>31</sup> Disk shaped charge-transfer (CT) complexes of HAT-TIm with

triphenylene (TPh: electron donors) have been reported recently.<sup>32</sup> Thus, combination of HAT-TIm and porphyrin seems to be ideal for fulfilling an enhanced light-harvesting efficiency of chromophores throughout the solar spectrum and efficient photoinduced electron transfer. However, photoinduced electron transfer of D-A supramolecular complexes with close contact of two large planar  $\pi$ -planes has yet to be examined.

We report herein ultrafast photoinduced electron transfer in supramolecular CT  $\pi$ -complexes formed between alkyl-substituted porphyrins and *N*-alkyl-substituted HAT-TIm with face-to-face close contact of two planar  $\pi$ -planes. First we examined and compared the electrochemical and photophysical properties of HAT and TPh derivatives (Chart 1). Then, the formation of strong HAT-TIm-porphyrin complexes and ultrafast photoinduced electron transfer in the complexes including alkyl chain dependencies are discussed in detail.

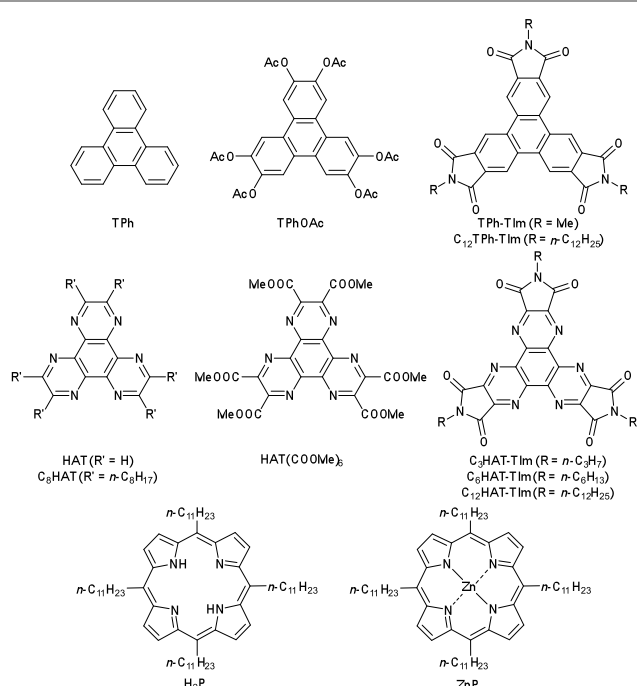


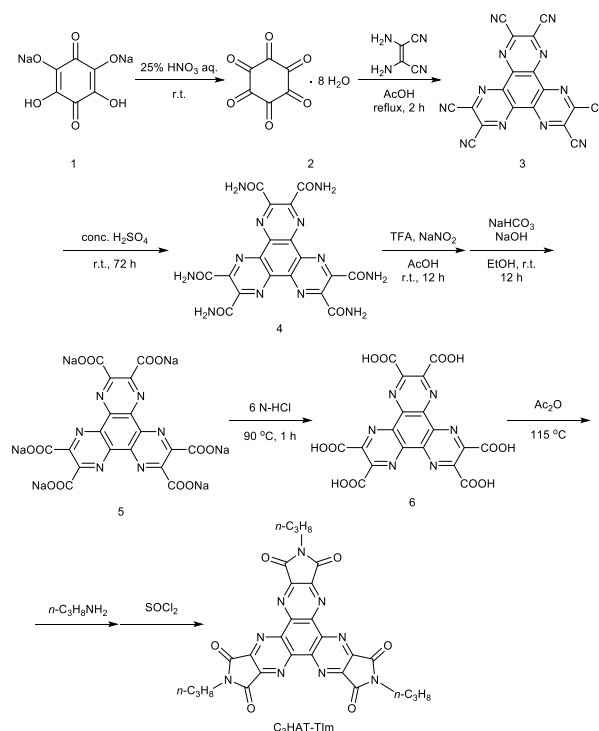
Chart 1 Chemical structures of TPh, HAT and porphyrin derivatives used in this study.

## Results and discussion

### Synthesis

HAT-TIm derivatives were synthesized according to the reported method by Kanakarajan and coworkers (Scheme 1).<sup>33,34</sup> Firstly, compound **1** was isomerized to compound **2** under acidic conditions. Next, dehydration condensation of compound **2** and 2,3-diaminomaleonitrile was carried out to prepare the HAT skeleton. Then, compound **4** was synthesized by acidic hydrolysis of compound **3**. To synthesize compound **5**, an HAT derivative **4** was reacted with TFA, NaNO<sub>2</sub> and AcOH, which was followed by the reaction under basic conditions.

Then, compound **6** was obtained by the reaction of compound **5** with 6 N-HCl at 90 °C, reacting with Ac<sub>2</sub>O at 115 °C, which was followed by the reaction with each alkyl amine. Finally, HAT-triimide derivatives were obtained by a reaction of the crude and thionyl chloride. HAT(COOMe)<sub>6</sub> was obtained by a reaction of compound **6** with MeOH and H<sub>2</sub>SO<sub>4</sub> according to the reported method.<sup>34</sup> The details of C<sub>3</sub>HAT-TIm (<sup>1</sup>H, <sup>13</sup>C NMR and MALDI-TOF mass spectra) were shown in Fig. S1-S3 (ESI<sup>†</sup>). H<sub>2</sub>P was synthesized by the reported literature<sup>35</sup> as shown in Scheme S1 (ESI<sup>†</sup>). Then, the synthesis of ZnP was achieved through the insertion of zinc into porphyrin center.



Scheme 1 Synthetic Schemes of C<sub>3</sub>HAT-TIm.

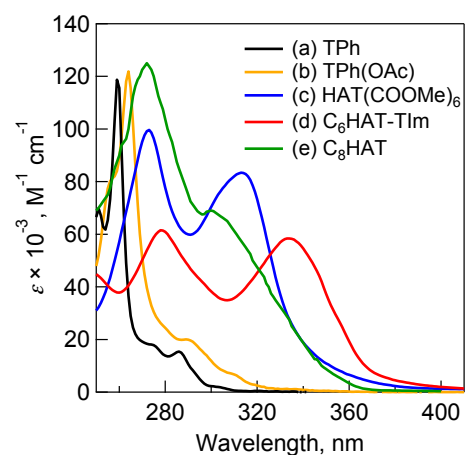


Fig. 1 Absorption spectra of (a) TPh (black), (b) TPhOAc (yellow), (c) HAT(COOMe)<sub>6</sub> (blue) and (d) C<sub>6</sub>HAT-TIm (red) in 10 μM CH<sub>2</sub>Cl<sub>2</sub>. (e) Normalized absorption spectrum of C<sub>6</sub>HAT (green) for comparison.<sup>36</sup>

### Steady-state spectroscopic measurements

Absorption spectra were measured to evaluate the electronic structures of HAT and TPh derivatives. Fig. 1 shows absorption spectra of TPh (spectrum *a*), TPhOAc (spectrum *b*), HAT(COOMe)<sub>6</sub> (spectrum *c*) and C<sub>3</sub>HAT-TIm (spectrum *d*) in CH<sub>2</sub>Cl<sub>2</sub>. The spectrum of C<sub>8</sub>HAT (spectrum *e*) is also shown for comparison although the  $\epsilon$  value is not calculated.<sup>36</sup> The spectra of TPh and TPhOAc have characteristic strong peaks at around 250-270 nm, whereas the peaks of HAT(COOMe)<sub>6</sub>, C<sub>3</sub>HAT-TIm and C<sub>8</sub>HAT become broadened and red-shifted. According to the electrochemical measurements and DFT calculations (Table 2), the red-shift trend may result from relatively low levels of LUMO states by introducing electron-withdrawing groups as compared to those of HOMO states, which leads to the decrease of HOMO-LUMO gap.<sup>37,38</sup>

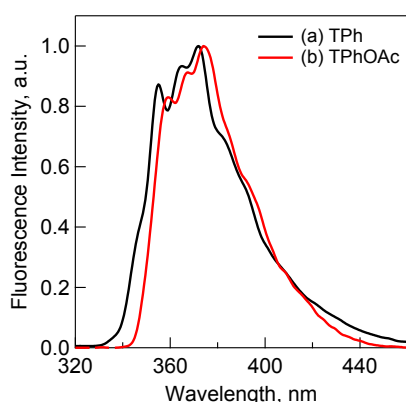


Fig. 2 Fluorescence spectra of (a) TPh (1.0  $\mu\text{M}$ ) (black) and (b) TPhOAc (1.0  $\mu\text{M}$ ) (red) in CH<sub>2</sub>Cl<sub>2</sub>.

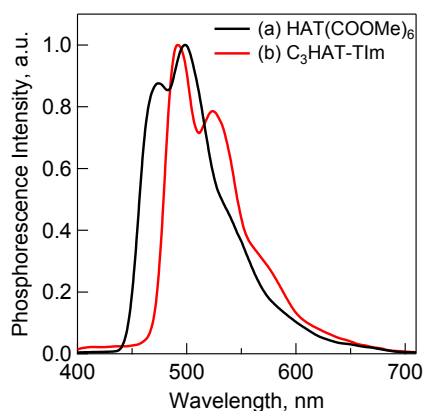


Fig. 3 Phosphorescence spectra of (a) HAT(COOMe)<sub>6</sub> (10  $\mu\text{M}$ ) and (b) C<sub>3</sub>HAT-TIm (50  $\mu\text{M}$ ) in MeCN. The excitation wavelength is 330 nm. The measurements were performed at 77 K.

The fluorescence spectra of TPh and TPhOAc (Fig. 2) show a fluorescence peak at ca. 355 nm, whereas the spectra of HAT(COOMe)<sub>6</sub> and C<sub>3</sub>HAT-TIm exhibit extremely small intensities. Consequently, we observed the corresponding phosphorescence spectra at 77 K as shown in Fig. 3. The energies of the triplet excited states of HAT(COOMe)<sub>6</sub> and C<sub>3</sub>HAT-TIm were determined from the phosphorescence

maxima, 474 nm and 492 nm, to be 2.61 eV and 2.52 eV, respectively. Additionally, phosphorescence lifetimes of HAT(COOMe)<sub>6</sub> and C<sub>3</sub>HAT-TIm (77 K) were determined to be 320 ms and 280 ms, respectively (Table 1). This suggests that intersystem crossing occurs efficiently in both compounds. The absorption and emission spectra of C<sub>6</sub>HAT-TIm and C<sub>12</sub>HAT-TIm are also very similar to those of C<sub>3</sub>HAT-TIm.

Table 1 Fluorescence parameters of TPh and HAT derivatives

compound	$\Phi_F$	$\Phi_{\text{Other}}$	$\tau_{\text{FL}}$ , ns	$\tau_{\text{PL}}$ , ms	$k_F \times 10^{-6}$ , s <sup>-1</sup>	$k_{\text{Other}} \times 10^{-7}$ , s <sup>-1</sup>
TPh	0.07 <sup>a</sup>	0.93	37 <sup>a</sup>	–	1.8	2.5
TPhOAc	0.13	0.87	9.4	–	14	9.3
HAT(COOMe) <sub>6</sub>	<0.01	>0.99	–	320	–	–
C <sub>3</sub> HAT-TIm	<0.01	>0.99	–	280	–	–

$\tau_{\text{FL}}$ : Fluorescence lifetime.  $\tau_{\text{PL}}$ : Phosphorescence lifetime (77 K).  $\Phi_F$ : Fluorescence emission quantum yield.  $\Phi_{\text{Other}}$ : Nonradiative quantum yield;  $\Phi_{\text{Other}} = 1 - \Phi_F$ ,  $k_F = \Phi_F \tau_{\text{FL}}^{-1}$ ,  $k_{\text{Other}} = \Phi_{\text{Other}} \tau_{\text{FL}}^{-1}$ . <sup>a</sup>Reported values.<sup>39</sup>

### Fluorescence quantum yields

To evaluate the detail light-emitting properties, we measured absolute fluorescence quantum yields ( $\Phi_F$ ) of these derivatives and the  $\Phi_F$  values are listed in Table 1. The  $\Phi_F$  value of TPhOAc ( $\Phi_F = 0.13$ ) is slightly larger than that of TPh ( $\Phi_F = 0.07$ ), whereas the  $\Phi_F$  values of HAT(COOMe)<sub>6</sub> and C<sub>3</sub>HAT-TIm are extremely low ( $\Phi_F$ : ~0). The low  $\Phi_F$  values of HAT(COOMe)<sub>6</sub> and C<sub>3</sub>HAT-TIm are consistent with the intensities of phosphorescence spectra in Fig. 3. This is attributable to the enhancement of intersystem crossing based on the spin-orbit coupling because of introduction of carbonyl groups.<sup>38</sup> The low  $\Phi_F$  and phosphorescence spectra of C<sub>6</sub>HAT-TIm and C<sub>12</sub>HAT-TIm were also similarly observed.

To further investigate and compare fluorescence properties between TPh and TPhOAc, fluorescence lifetime measurements of these derivatives were performed. The fluorescence decays were examined in CH<sub>2</sub>Cl<sub>2</sub> using the pulsed 404 nm laser light, which excited these moieties. The fluorescence lifetimes ( $\tau_{\text{FL}}$ ) were evaluated from a monoexponential fitting for the respective compounds and the  $\tau_{\text{FL}}$  values are listed in Table 1. The  $\tau_{\text{FL}}$  value of TPhOAc (9.4 ns) is much shorter than that of TPh (37 ns). To discuss the excited dynamics carefully, the net rate constants of the above two processes such as fluorescence emission ( $k_F$ ) and other processes ( $k_{\text{Other}}$ ) were determined as shown in Table 2. The  $k_F$  value of TPhOAc is by one order of magnitude greater than that of TPh. Additionally, in both freebase and zinc porphyrins (e.g., tetraphenylporphyrin), the quantum yields of intersystem crossing ( $\Phi_{\text{ISC}}$ : ca. 0.8 ~ 0.9) are much larger than those of fluorescence pathways ( $\Phi_F$ : ca. 0.05 ~ 0.10).<sup>39b</sup> Based on these results, we can conclude that introduction of substituents successfully contributes to the improvement of light-emitting property of TPh derivatives.

### Electrochemical studies and DFT calculations

Electrochemical behaviors of TPh and HAT derivatives were investigated by cyclic voltammetry

Table 2 Redox potentials and HOMO/LUMO energies of TPh and HAT derivatives

compound	$E_{\text{red1}}^a$	$E_{\text{red2}}^a$	$E_{\text{red3}}^a$	$E_{\text{ox}}^a$	HOMO, eV <sup>g</sup>	LUMO, eV <sup>g</sup>	gap, eV
TPh	-2.42 <sup>b</sup>	–	–	1.64 <sup>c</sup>	-5.89	-0.92	4.97
TPhOAc	-2.19 <sup>d</sup>	–	–	1.63 <sup>c</sup>	-6.20	-1.54	4.66
C <sub>12</sub> TPh-TIm	-1.21 <sup>e</sup>	–	–	–	-7.31	-3.25	4.06
HAT	-1.42 <sup>f</sup>	-1.72 <sup>f</sup>	–	–	-6.89	-2.16	4.73
HAT(COOMe) <sub>6</sub>	-0.59	-1.08	–	–	-7.58	-3.43	4.15
C <sub>6</sub> HAT-TIm	-0.39	-0.85	-1.21	–	-7.54	-3.63	3.91

<sup>a</sup> V vs SCE in CH<sub>2</sub>Cl<sub>2</sub>. <sup>b</sup> Reported value in dimethylamine/THF<sup>40</sup> <sup>c</sup> Reported value.<sup>41</sup> <sup>d</sup> Determined by differential pulse voltammetry (DPV) in THF. <sup>e</sup> Reported value in CH<sub>2</sub>Cl<sub>2</sub>.<sup>42</sup> <sup>f</sup> Reported value in MeCN.<sup>43</sup> <sup>g</sup> Calculated by B3LYP/6-31+G(d) level.

to examine the substituent effects on the reduction and oxidation potentials. The representative voltammograms of HAT(COOMe)<sub>6</sub> and C<sub>6</sub>HAT-TIm in DMF or CH<sub>2</sub>Cl<sub>2</sub> containing 0.10 M tetra-*n*-butylammonium hexafluorophosphate (*n*-Bu<sub>4</sub>NPF<sub>6</sub>) are shown in Fig. 4. The measured half-wave potentials of these compounds together with reference TPh and HAT are listed in Table 1. The first reduction ( $E_{\text{red1}}$ ) and oxidation ( $E_{\text{ox}}$ ) potentials of TPh were reported to be -2.42 V and +1.64 V against saturated calomel electrode (SCE).<sup>40,41</sup> Similarly, we determined the first reduction potentials of TPhOAc ( $E_{\text{red1}} = -2.19$  V), HAT ( $E_{\text{red1}} = -1.42$  V),<sup>42</sup> C<sub>12</sub>TPh-TIm ( $E_{\text{red1}} = -1.42$  V),<sup>43</sup> HAT(COOMe)<sub>6</sub> ( $E_{\text{red1}} = -0.59$  V) and C<sub>6</sub>HAT-TIm ( $E_{\text{red1}} = -0.39$  V). However, no corresponding oxidation potentials of HAT derivatives could be determined because of the higher oxidation potentials than the solvent. The  $E_{\text{red1}}$  value of C<sub>6</sub>HAT-TIm is quite similar to those of C<sub>3</sub>HAT-TIm ( $E_{\text{red1}} = -0.39$  V) and C<sub>12</sub>HAT-TIm ( $E_{\text{red1}} = -0.40$  V) as shown in ESI (Fig. S4†). With increasing the number of electron-withdrawing groups such as pyrazine, COOMe, OAc and imide units, the successive positive shifts of reduction potentials were observed. In particular, the  $E_{\text{red1}}$  value of HAT-TIm is quite comparable to that of C<sub>60</sub> (-0.44 V vs SCE),<sup>31</sup> which indicates that HAT-TIm is a good electron acceptor.

Moreover, the cyclic voltammogram of C<sub>6</sub>HAT-TIm exhibits the further reduction up to trianions, C<sub>6</sub>HAT-TIm<sup>3-</sup>. The HOMO and LUMO levels calculated by DFT method (Fig. S5 and Fig. S6†) also support the above trends observed in electrochemical data in Table 2. Namely, these shifts of HOMO and LUMO levels are largely dependent on the electron-withdrawing nature and the number of substituents. Additionally, the LUMO of HAT-TIm is energetically low lying and doubly degenerate, and thus capable of accepting three electrons upon reduction (Fig. 4).

With regard to the porphyrin derivatives such as H<sub>2</sub>P and ZnP, the first oxidation potentials of H<sub>2</sub>P and ZnP were determined to be +0.78 V and +0.68 V, respectively (Fig. S7 in ESI†). The energy level of the charge-separated state of HAT-TIm and porphyrin (e.g., ZnP) composites (i.e., HAT-TIm radical anion and ZnP radical cation) was determined from the difference between  $E_{\text{ox}}$  of ZnP and  $E_{\text{red1}}$  of HAT-TIm (-0.39 V vs SCE) to be 1.07 eV. This value is smaller than the excited energies of each chromophore: ~2.1 eV and ~1.5 eV for the singlet and triplet excited states of ZnP,<sup>44</sup> respectively, and ~3.7

eV and 2.52 eV for the singlet and triplet excited states of HAT-TIm, respectively. Thus, photoinduced electron transfer from the excited state of ZnP to HAT-TIm and/or ZnP to the excited state of HAT-TIm are energetically favorable because the free energy changes of photoinduced electron transfer are always negative. In such a case, the combination between porphyrin and HAT-TIm units is expected to perform the efficient photoinduced electron transfer to form the charge-separated state (*vide infra*).

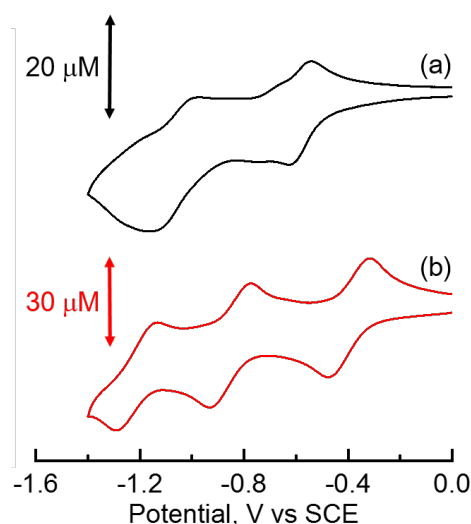


Fig. 4 Cyclic voltammograms of (a) HAT(COOMe)<sub>6</sub> in DMF and (b) C<sub>6</sub>HAT-TIm in CH<sub>2</sub>Cl<sub>2</sub> with 0.10 M *n*-Bu<sub>4</sub>NPF<sub>6</sub> as supporting electrolyte. Reference electrode: standard calomel electrode. Scan rate: 0.10 V/s.

#### Spectroscopic characterization of reduced C<sub>3</sub>HAT-TIm

When the dimeric 1-benzyl-1,4-dihydronicotinamide [(BNA)<sub>2</sub>] is used as an electron donor,<sup>45,46</sup> irradiation of a CH<sub>2</sub>Cl<sub>2</sub> solution containing (BNA)<sub>2</sub> and C<sub>3</sub>HAT-TIm with visible light resulted in the photoinduced one-electron reduction of C<sub>3</sub>HAT-TIm to produce C<sub>3</sub>HAT-TIm<sup>•-</sup>. Fig. 5 shows the absorption spectral change in the photoinduced electron-transfer reduction of C<sub>3</sub>HAT-TIm to C<sub>3</sub>HAT-TIm<sup>•-</sup>. In this case, a new absorption band at  $\lambda_{\text{max}} = 482$  nm with a broad near-IR absorption band at 800 nm appeared, corresponding to the radical anion species. The molar absorption coefficient of C<sub>3</sub>HAT-TIm<sup>•-</sup> was determined to be  $6.2 \times 10^3 \text{ M}^{-1} \text{ cm}^{-1}$  at 482 nm.

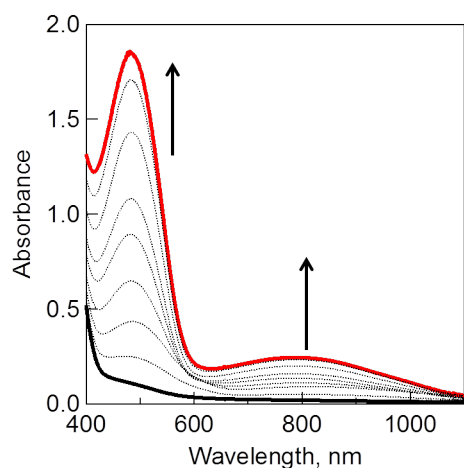
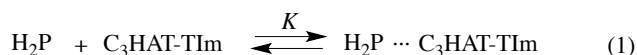


Fig. 5 UV-vis spectral changes observed in photoinduced electron-transfer reduction of C<sub>3</sub>HAT-TIm (300 μM) with (BNA)<sub>2</sub> (150 μM) in deaerated CH<sub>2</sub>Cl<sub>2</sub> at 298 K under photoirradiation with a xenon lamp.

### Formation constants of CT complexes between HAT-TIm and porphyrins

CT complex formation between HAT-TIm and H<sub>2</sub>P was examined by the absorption spectral changes (Fig. 6). The absorption of original Soret band of H<sub>2</sub>P at 418 nm decreased and a strong absorption peak newly appeared at around 440 nm due to the complexation of C<sub>3</sub>HAT-TIm with H<sub>2</sub>P in CH<sub>2</sub>Cl<sub>2</sub> as shown in Fig. 6A, where the inserted figure clearly indicates formation of the typical CT  $\pi$ -complex between H<sub>2</sub>P and C<sub>3</sub>HAT-TIm. The CT complex absorption extends up to ~800 nm (ESI Fig. S8†). The Job's plot in Fig. 7 exhibits a triangle-like shape with a maximum value 0.48, which indicates that a 1 : 1 complex (theoretical maximum: 0.50) is formed between H<sub>2</sub>P and C<sub>3</sub>HAT-TIm (eq 1).



$$(\alpha^{-1} - 1)^{-1} = K ([\text{C}_3\text{HAT-TIm}] - \alpha[\text{H}_2\text{P}]_0) \quad (2)$$

$$\alpha = (A - A_0)/(A_\infty - A_0) \quad (3)$$

The formation constant ( $K$ ) was determined by a linear correlation between  $(\alpha^{-1} - 1)^{-1}$  and  $([\text{C}_3\text{HAT-TIm}] - \alpha[\text{H}_2\text{P}]_0)$  in eqs 2 and 3, where  $A_0$  and  $A$  are the absorbance of H<sub>2</sub>P at 424 nm in the absence and presence of C<sub>3</sub>HAT-TIm, and  $[\text{H}_2\text{P}]_0$  is the initial concentration of H<sub>2</sub>P. From a linear plot in the inset of Fig. 6B, the formation constant ( $K$ ) of the H<sub>2</sub>P–C<sub>3</sub>HAT-TIm complex was determined to be  $1.4 \times 10^4 \text{ M}^{-1}$  in CH<sub>2</sub>Cl<sub>2</sub> (Fig. 6B). As H<sub>2</sub>P forms the CT complex with HAT-TIm, the fluorescence emission of H<sub>2</sub>P was quenched by intramolecular electron transfer from the singlet excited state of H<sub>2</sub>P to C<sub>3</sub>HAT-TIm in the complex (Fig. 8A).

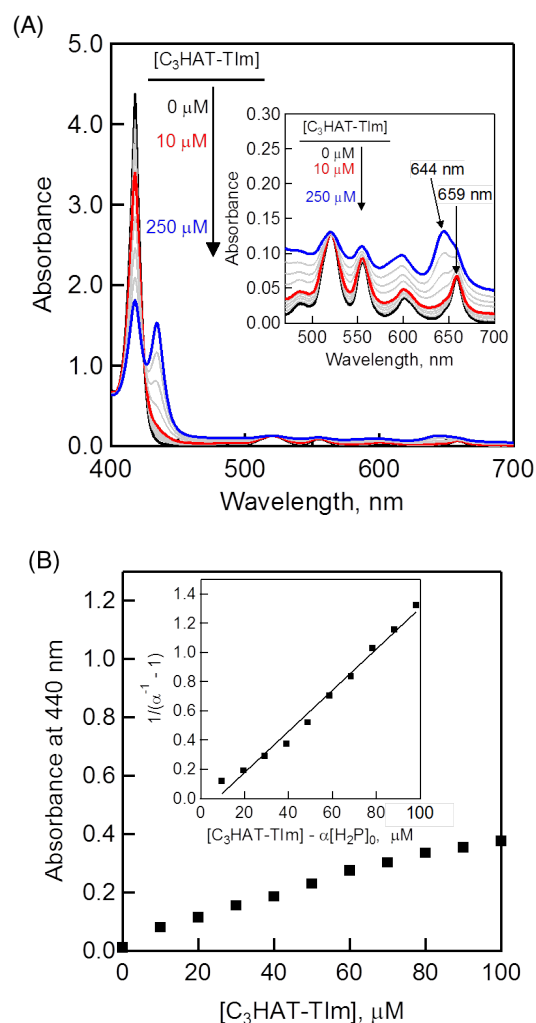


Fig. 6 (A) Absorption spectral changes of H<sub>2</sub>P ([H<sub>2</sub>P] = 10 μM) upon addition of C<sub>3</sub>HAT-TIm (0 μM - 100 μM) in CH<sub>2</sub>Cl<sub>2</sub>. The inserted expanded Fig. indicates a broad CT absorption of the H<sub>2</sub>P–C<sub>3</sub>HAT-TIm coplex. (B) Absorption profile at 440 nm. Inset: Plot of  $(\alpha^{-1} - 1)^{-1}$  vs  $([\text{C}_3\text{HAT-TIm}] - \alpha[\text{H}_2\text{P}]_0)$ .

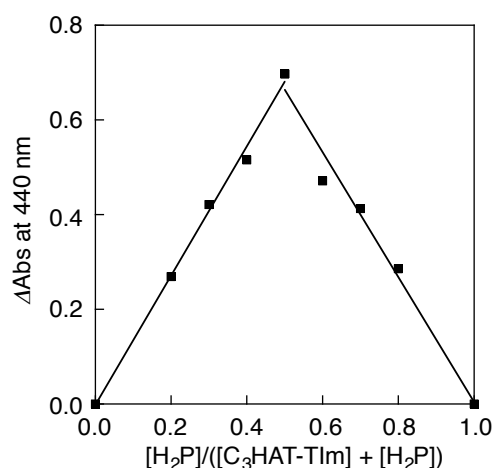


Fig. 7 Job's plot obtained by absorption change at 440 nm for the complex formation between H<sub>2</sub>P and C<sub>3</sub>HAT-TIm. Symmetric plot with maxima at 0.5 mole fraction indicates formation of the 1 : 1 complex in the present system.

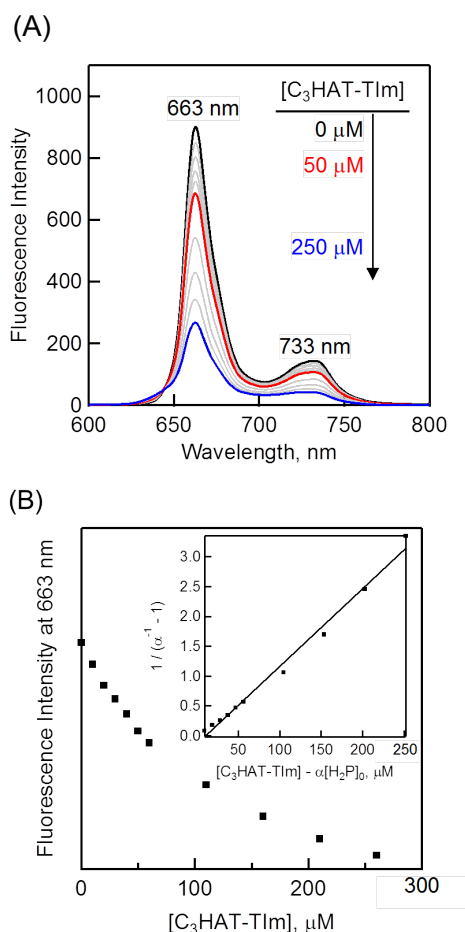


Fig. 8 (A) Fluorescence spectral changes of  $H_2P$  ( $[H_2P] = 10 \mu M$ ) upon addition of increasing equivalents of  $C_3HAT-TIm$  ( $0 \mu M - 250 \mu M$ ) in  $CH_2Cl_2$ . Excitation wavelength:  $550 \text{ nm}$ . (B) Plot of the fluorescence intensity vs  $[C_3HAT-TIm]$  at  $663 \text{ nm}$ . Inset: Plot of  $(\alpha^{-1} - 1)^{-1}$  vs  $[C_3HAT-TIm] - \alpha[H_2P]_0$  according to eqs 2 and 3.

Table 3 Formation constants determined by fluorescence titration of  $H_2P/ZnP$  and  $HAT-TIm$  derivatives in  $CH_2Cl_2$

HAT-TIm	$K(H_2P), M^{-1}$	$K(ZnP), M^{-1}$
$C_3HAT-TIm$	$1.3 \times 10^4$	$3.0 \times 10^3$
$C_6HAT-TIm$	$2.1 \times 10^4$	$6.5 \times 10^3$
$C_{12}HAT-TIm$	$1.8 \times 10^4$	$5.2 \times 10^3$

The formation constant  $K$  of  $H_2P-C_3HAT-TIm$  complex was determined from the changes in the fluorescence intensities at  $663 \text{ nm}$  (Fig. 8B) to be  $1.3 \times 10^4 M^{-1}$ , which agrees with the value determined from the absorption spectral change in Fig. 6B.<sup>47</sup> The formation constants  $K$  between porphyrins (i.e.,  $H_2P$  and  $ZnP$ ) and  $HAT-TIm$  derivatives are summarized in Table 3. The largest value of formation constant  $K$  was obtained for  $H_2P-C_6HAT-TIm$  as  $2.1 \times 10^4 M^{-1}$ . The longer alkyl chain unit may enhance the CT  $\pi$ -complex formation because of the additional van der Waals interaction. This is similar to that obtained for  $H_2P-C_{12}HAT$  (Figs. S9 and S10 in ESI<sup>†</sup>). When  $H_2P$  was replaced by  $ZnP$ , the formation constants became smaller (Table 3 and Figs. S11-S13 in ESI<sup>†</sup>).

### $^1H$ NMR titration

The  $^1H$  NMR signals of  $H_2P$  exhibit upfield shifts of  $\beta$  protons upon the complexation with  $HAT-TIm$  as shown in Fig. 9. This is ascribed to the influence of the large porphyrin aromatic ring current. This result indicates that the two-dimensional  $\pi$ -structure of  $HAT-TIm$  interacts with that of  $H_2P$ .

The signal of the free  $H_2P$  and the complexed  $H_2P$  always coalesce into a single signal. This indicates that the complexation and exchange occur at a faster rate than the NMR time scale. The formation constant between  $H_2P$  and  $HAT-TIm$  was determined from the peak shifts of  $\beta$  protons in  $H_2P$  moiety using the following eq 4:<sup>48</sup>

$$\Delta\delta = \frac{\Delta\delta_{\max}}{-R_0} \left[ \frac{[s_0]}{2} + \frac{\Sigma}{2} \left[ 1 - \sqrt{1 + \frac{[s_0]^2 - 2[s_0]\Psi}{\Sigma^2}} \right] \right] \quad (4)$$

$$\Sigma = [R_0] + \frac{1}{K_a} \quad \Psi = [R_0] - \frac{1}{K_a}$$

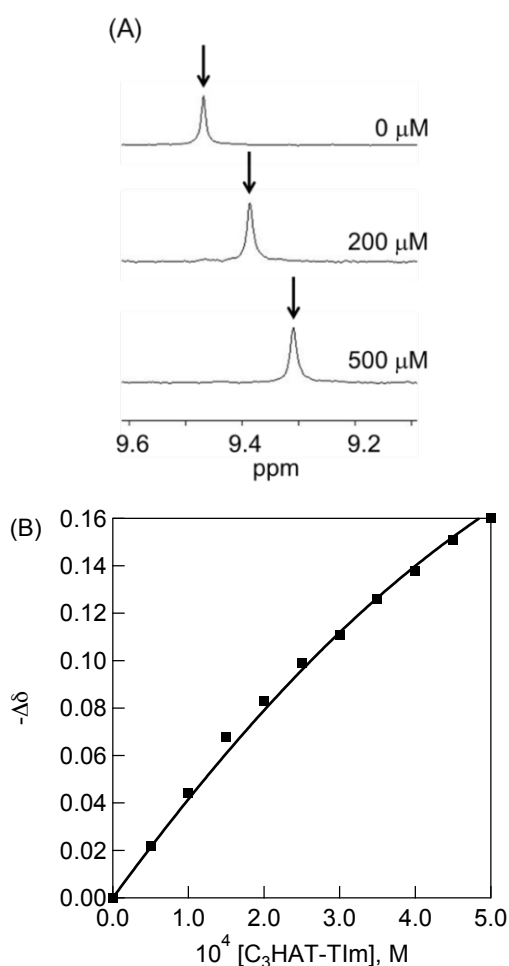


Fig. 9 (A)  $^1H$  NMR titration of  $H_2P$  ( $[H_2P] = 500 \mu M$ ) upon addition of  $C_3HAT-TIm$  ( $0 \mu M - 500 \mu M$ ) in  $CDCl_3$ . (B)  $^1H$  NMR titration curve obtained from the chemical shift changes of  $\beta$  proton of  $H_2P$  by adding  $C_3HAT-TIm$ .

where  $\Delta\delta$  is the observed change in chemical shift,  $\Delta\delta_{\max}$  is the saturation value,  $S_0$  and  $R_0$  are the total concentrations of guest and receptor, respectively.

A sample titration curve can be seen in the case of  $C_3HAT-TIm$  as the guest (Fig. 9B), and the formation constant was determined to be  $5.1 \times 10^3 M^{-1}$ . Similarly, the formation constant of  $H_2P-C_6HAT-TIm$  was determined to be  $8.9 \times 10^3 M^{-1}$  (Fig. S14 in ESI†). The formation constants between porphyrins and HAT-TIm derivatives in  $CDCl_3$  increase with increasing alkyl chain lengths as observed in spectroscopic measurements in  $CH_2Cl_2$ . The  $K$  values in  $CDCl_3$  are somewhat smaller than those in  $CH_2Cl_2$  due to the less stabilization of CT complexes in the less polar solvent ( $CDCl_3$ ).

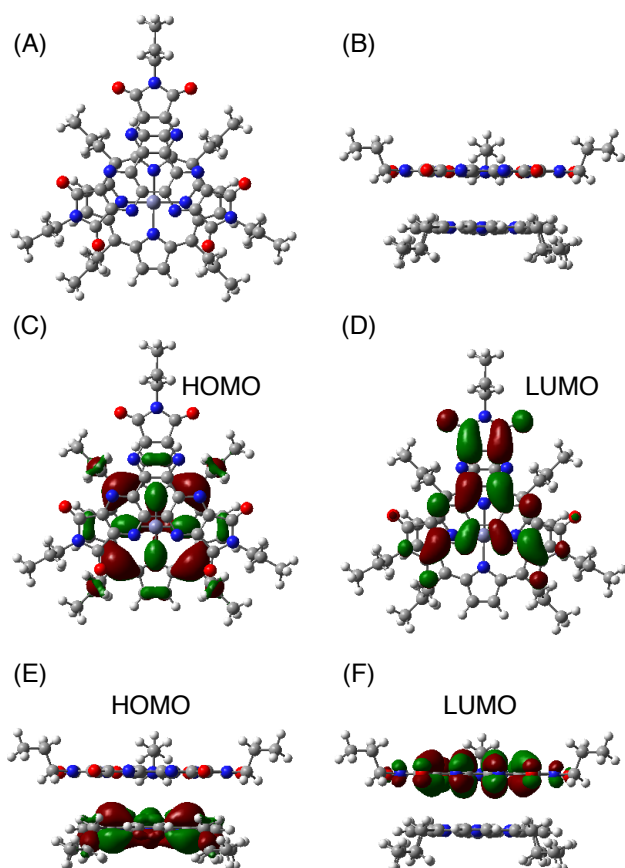


Fig. 10 B3LYP/6-31G(d) optimized structure of ZnP and  $C_3HAT-TIm$  (A and B). The HOMO and LUMO of the  $\pi$ -complex are shown in top view (C and D) and side view (E and F), respectively. In ZnP, 11-carbon alkyl chains were replaced with 3-carbon chains for saving computing time.

### DFT computational studies of supramolecular CT $\pi$ -complexes

DFT calculations also support the CT  $\pi$ -complex formation between porphyrin and HAT-TIm units. Fig. 10A and 10B show the face-to-face planar structure of the CT complex composed of ZnP and  $C_3HAT-TIm$ . The distance between porphyrin and HAT units is found to be 3.8 Å. The calculated HOMO and LUMO orbitals of the CT  $\pi$ -complex are localized on porphyrin and HAT-TIm units, respectively (Fig. 10C-F).<sup>49</sup> The similar trend was observed in case of ZnP and  $C_3HAT-TIm$ .

TD-DFT calculation for ZnP- $C_3HAT-TIm$  was carried out using the TD-B3LYP/6-31G(d)//B3LYP/6-31G(d) basis set to assign the absorption band at NIR region ( $\lambda_{\max} = 800$  nm, Fig. 6A and Fig. S8).<sup>50</sup> The calculated absorption band was obtained at 815 nm with an oscillator strength of  $f = 0.172$ , ascribable to charge transfer from the ZnP moiety to the  $C_3HAT-TIm$  moiety. The calculated results are shown in S15 (ESI†). We also carried out TD-DFT calculations of ZnP and  $C_3HAT-TIm$  as references, indicating no absorption band was obtained at NIR region (S15-S17 in ESI†).

### Ultrafast photoinduced electron transfer in CT $\pi$ -complexes between porphyrins and HAT-TIm

The occurrence of ultrafast electron transfer from the singlet excited states of porphyrins to HAT-TIm in the complexes was further confirmed by femtosecond laser-induced transient absorption measurements. Transient absorption spectra of pristine  $H_2P$  in toluene using 430 nm laser pulse, which selectively excited only porphyrin units, show the singlet-singlet transient absorption and fluorescence bleaching bands (ca. 660 nm) of  $H_2P$  (Fig. 11A). In case of  $H_2P-C_3HAT-TIm$ , we employed a large excess concentration of  $C_3HAT-TIm$  (8 mM) relative to that of  $H_2P$  to make sure that all  $H_2P$  molecules form the CT complex with  $C_3HAT-TIm$  (> 99%) in Fig. 11B. The transient absorption spectra of  $H_2P-C_3HAT-TIm$  exhibit a broad absorption in the ca. 600-700 nm region within 1 ps after laser pulse excitation due to  $H_2P^{*+}$ ,<sup>44,51</sup> without fluorescence bleaching at ca. 660 nm (Fig. 11B). The radical anion species of  $C_3HAT-TIm$  is also seen at around 500 nm region by comparing the absorption spectrum of reduced  $C_3HAT-TIm$  (Fig. 5).

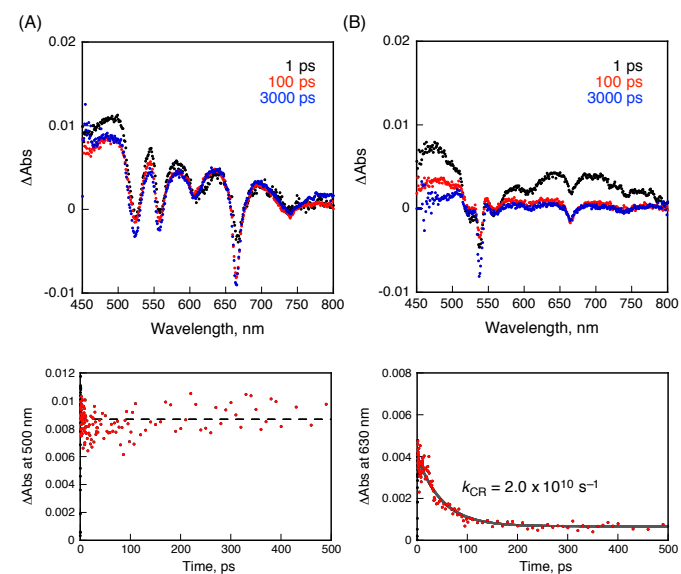


Fig. 11 Femtosecond laser-induced transient absorption spectra and corresponding time profiles of (A)  $H_2P$  and (B)  $H_2P-C_3HAT-TIm$  obtained at 1.0 ps (black), 100 ps (red) and 3000 ps (blue) after laser pulse in toluene. The time profiles were detected at 500 and 630 nm, respectively. The concentrations of  $H_2P$  and  $C_3HAT-TIm$  are 10  $\mu M$  and 8.0 mM, respectively. Excitation wavelength is 430 nm.



This indicates that photoinduced charge separation occurs immediately within 1 ps upon photoexcitation of the charge-transfer without showing the singlet-singlet transient absorption due to  $^1\text{H}_2\text{P}^*$ . Such ultrafast charge separation is unprecedented for supramolecular electron donor-acceptor complexes,<sup>12,17-22,52-54</sup> resulting from a strong interaction between  $\text{H}_2\text{P}$  and  $\text{HAT-TIm}$  derivative in the face-to-face planar structure in the CT  $\pi$ -complex (Fig. 10B).

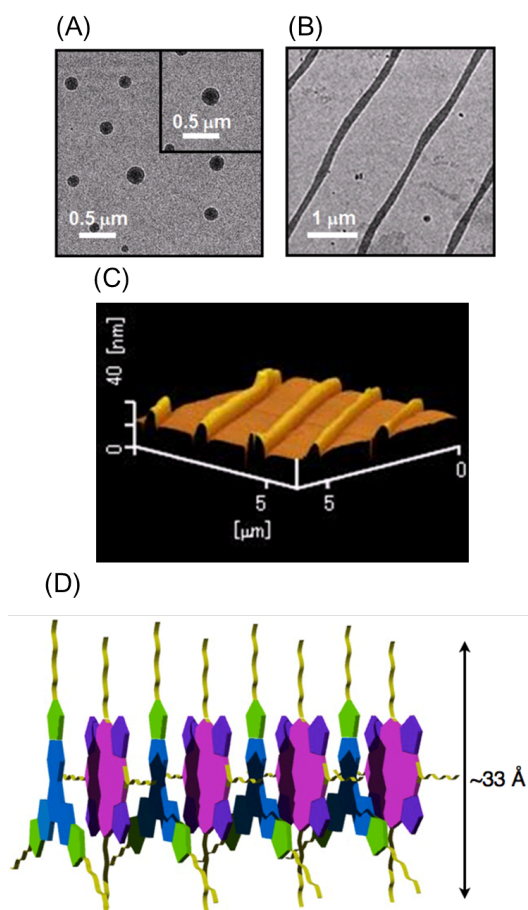


Fig. 12 TEM images of (A)  $\text{C}_3\text{HAT-TIm}$  assembly and (B)  $\text{H}_2\text{P-C}_3\text{HAT-TIm}$  assembly. The images were taken by drop cast of the  $\text{CH}_2\text{Cl}_2$  solution of the components onto the grid. (C) AFM image of  $\text{H}_2\text{P-C}_3\text{HAT-TIm}$  composites. (D) Schematic illustration of proposed supramolecular structures between  $\text{H}_2\text{P}$  (pink/purple) and  $\text{C}_3\text{HAT-TIm}$  (blue/green).

The charge-recombination dynamics were monitored from the decay of the transient absorption at 630 nm due to the  $\text{H}_2\text{P}^{++}$  as shown in Fig. 11B. The rate constant of the charge recombination ( $k_{\text{CR}}$ ) is determined to be  $2.0 \times 10^{10} \text{ s}^{-1}$ . A similar  $k_{\text{CR}}$  value ( $2.2 \times 10^{10} \text{ s}^{-1}$ ) was obtained for the  $\text{H}_2\text{P-C}_6\text{HAT-TIm}$  complex as shown in Fig. S18 (ESI $^\dagger$ ). Additionally, the transient spectra of  $\text{ZnP}$  and  $\text{ZnP-C}_3\text{HAT-TIm}$  are shown in ESI Fig. S19 $^\dagger$ . However, photoinduced charge separation of  $\text{ZnP-C}_3\text{HAT-TIm}$  was not confirmed under our experimental set-up. This is probably attributable to

the smaller formation constant ( $K = 3.0 \times 10^3 \text{ M}^{-1}$ ) than that of  $\text{H}_2\text{P-C}_3\text{HAT-TIm}$  ( $K = 1.3 \times 10^4 \text{ M}^{-1}$ ) as shown in Table 1.

### High-order organization of the $\text{H}_2\text{P-C}_3\text{HAT-TIm}$ complex observed by TEM and AFM

Evaporation of the solvent of a  $\text{CH}_2\text{Cl}_2$  solution of the  $\text{H}_2\text{P-C}_3\text{HAT-TIm}$  complex resulted in high-order supramolecular organization, which was observed by TEM and AFM. The supramolecular organization patterns composed of  $\text{C}_3\text{HAT-TIm}$  and  $\text{H}_2\text{P}$  were obtained by the following method.<sup>55</sup> First, we optimized the experimental condition (10  $\mu\text{M}$   $\text{CH}_2\text{Cl}_2$  solution of  $\text{C}_3\text{HAT-TIm}$  and  $\text{H}_2\text{P}$ ) by examining the concentration effect (5-50  $\mu\text{M}$ ) on the aggregate structures. Then, the solution (the optimized concentration: 10  $\mu\text{M}$ ) was simply cast onto the carbon-coated copper film (TEM grid) and dried in air. In the evaporation process of solvent, the linear molecular pattern was effectively formed. The assemblies of  $\text{C}_3\text{HAT-TIm}$  reference system were also prepared in the same manner. TEM measurements of  $\text{C}_3\text{HAT-TIm}$  reference system without porphyrins showed many spherical assemblies (Fig. 12A), whereas aligned fibrous patterns (linear aggregates) were observed for the  $\text{H}_2\text{P-C}_3\text{HAT-TIm}$  complex (Fig. 12B). The approximate average width of  $\text{H}_2\text{P-C}_3\text{HAT-TIm}$  assemblies was estimated to be  $\sim 200 \text{ nm}$ . AFM measurements including the cross-sectional height information were also performed as shown in Fig. 12C. In the AFM image, we could see the surface patterning, which is very similar to the corresponding TEM images (Fig. 12B). The cross-sectional data showed the average height: 10.1 nm. Considering the chemical structure of  $\text{H}_2\text{P}$  (approximate molecular size:  $\sim 33 \text{ \AA}$  estimated by DFT method) in Fig. 12D, the average height approximately corresponds to a few layers of  $\text{H}_2\text{P-C}_3\text{HAT-TIm}$  composite units.

### Conclusions

The present study has demonstrated formation of face-to-face 1:1 CT  $\pi$ -complexes between 1,4,5,8,9,12-hexaazatriphenylene (HAT) derivatives and porphyrins, which undergo ultrafast photoinduced electron transfer in which HAT derivatives with electron-withdrawing groups act as a good electron acceptor. Such unprecedented ultrafast charge-separated states were successfully formed by CT  $\pi$ -complexes. The CT  $\pi$ -complexes also contribute to the highly ordered patterning on the solid-state film. Such a simple method for molecular organization provides a new perspective for the construction and development of efficient molecular electronic and energy conversion systems.

### Experimental section

#### General information

Triphenylene and hexaacetoxyporphyrin were purchased from Tokyo Chemical Industry (TCI). They were used after reprecipitation from dichloromethane and hexane for spectroscopic and electrochemical measurements. All solvents and reagents of the best grade available were purchased from

commercial suppliers and were used without further purification. Column flash chromatography was performed on silica gel (Kanto Chemical Silica gel 60N, 40-50 mm or 100-210 mm). We used an LC-9204 apparatus equipped with a pump (JAI PI-60, flow rate 2.5 mL / min), a UV detector (JAI UV-3740) and two columns (JAIGEL 2H and 1H, 40 × 600 mm for each). All experiments except single crystal X-ray diffraction measurements were performed at room temperature. <sup>1</sup>H NMR and <sup>13</sup>C NMR spectra were recorded on a 400 MHz spectrometer JEOL JNM-A400, JNM-AI400, or JNM-ECX 400, using the solvent peak as the reference standard, with chemical shifts given in parts per million. CDCl<sub>3</sub> was used as a solvent for NMR measurements. MALDI-TOF mass spectra were recorded on a Bruker Ultra flex.

### Electrochemical measurements

Cyclic voltammograms were recorded on an Iviumstat 20 V / 2.5 A potentiostat by using a three electrode system. A platinum electrode was used as the working electrode. A platinum wire served as the counter electrode, and a saturated calomel electrode was used as the reference electrode. Ferrocene/ferrocenium redox couple was used as an internal standard. All the solutions were purged by using nitrogen gas prior to electrochemical and spectral measurements.

### Spectroscopic measurements

UV/Vis absorption spectra were recorded on a Perkin Elmer (Lambda 750) UV-VIS-NIR spectrophotometer. Fluorescence and phosphorescence emission spectra were recorded on a Parkin Elmer (LS-55) spectrofluorophotometer. Fluorescence lifetimes were measured on a HORIBA Scientific time-correlated single-photon counting system (FluoroCube) with the laser light (DeltaDiode, laser diode head, 404 nm, pulse width: 100 ps) as an excitation source. Phosphorescence lifetimes were measured on a JASCO FP-8500. The absolute fluorescence quantum yields were determined by a Hamamatsu Photonics C9920-02 system equipped with an integrating sphere and a red-sensitive multichannel photodetector (PMA-12): excitation wavelength = 300 nm.

### Laser flash photolysis measurements

Femtosecond laser-induced transient absorption measurements were conducted using an ultrafast source: Integra-C (Quantronix Corp.) and a commercially available optical detection system: Helios provided by Ultrafast Systems LLC. The detailed instrumentations are given in ESI†.

### Synthesis of C<sub>3</sub>HAT-TIm

HAT **6** (0.52 mol, 0.26 g) was dissolved to acetic anhydride (15 mL), and the solution was stirred for 15 min at 115 °C. After evaporation of the solvent, the resulting solid was dissolved to acetonitrile (20 mL). Then, *n*-propylamine (12.2 mol, 1 mL) was injected to the mixture solution with a syringe when the precipitation immediately arose. The resulting solid was collected by filtration. The solid was dissolved to thionyl chloride (10 mL), and the solution was stirred for 12 h at room

temperature. After evaporation of thionyl chloride, flash column chromatography on silica gel with chloroform/methanol (1: 1 v/v) as the eluent afforded C<sub>3</sub>HAT-TIm. Yield: 0.23 g (77.4%). <sup>1</sup>H NMR (400 MHz, CDCl<sub>3</sub>): δ = 3.83 (t, *J* = 7.1 Hz, 2 H, NCH<sub>2</sub>), 1.78 (dd, *J* = 7.3 Hz, 7.6 Hz, 2H, CH<sub>2</sub>), 1.02 (t, *J* = 7.6 Hz, 3 H, CH<sub>3</sub>); <sup>13</sup>C NMR (98.5 MHz, CDCl<sub>3</sub>): δ = 164.1 (C<sub>Ar</sub>), 149.0 (C<sub>Ar</sub>), 143.8 (C<sub>Ar</sub>), 40.1 (C<sub>Al</sub>), 21.3 (C<sub>Al</sub>), 11.4 (C<sub>Al</sub>); MALDI-TOF MS: calcd. for C<sub>27</sub>H<sub>21</sub>N<sub>9</sub>O<sub>6</sub>: 567.16, found 567.18 [M]. <sup>1</sup>H NMR, <sup>13</sup>C NMR and MALDI-TOF mass spectra are shown in ESI Fig. S1- S3†.

### Theoretical calculations

Density functional theory (DFT) calculations of ZnP-C<sub>3</sub>HAT-TIm, ZnP and C<sub>3</sub>HAT-TIm were performed with Gaussian 09 (Revision A.02, Gaussian, Inc.). The calculations were performed on a 32-processor QuantumCubeTM at the B3LYP/6-31G(d) level of theory.<sup>56</sup> Graphical outputs of the computational results were generated with the GaussView software program (ver. 3.09) developed by Semichem, Inc.<sup>57</sup> Electronic excitation energies and intensities were computed by the time-dependent (TD)-DFT calculation at the B3LYP/6-31G(d) level. The size of the integration grid used for all calculation was 4. In each case, 30 excited states were calculated by including all one-electron excitations within an energy window of ±3 hartrees with respect to the HOMO/LUMO energies.

### Acknowledgements

This work was partially supported by Grant-in-Aid for Scientific Research (Nos. 26286017 & 26620159 to T.H., Nos. 26620154 & 26288037 to K.O., No. 26102012 to T.T.) and the Science Research Promotion Fund from the Promotion and Mutual Aid Corporation for Private Schools from MEXT, Japan, and Mitsubishi Foundation.

### Notes and references

<sup>a</sup> Department of Chemistry, Faculty of Science and Technology, Keio University, Yokohama, 223-8522, Japan. E-mail: hasobe@chem.keio.ac.jp

<sup>b</sup> Department of Material and Life Science, Graduate School of Engineering, Osaka University, ALCA, Japan Science and Technology Agency (JST), Suita, Osaka, 565-0871, Japan. E-mail: fukuzumi@chem.eng.osaka-u.ac.jp

<sup>c</sup> Department of Applied Physics, Waseda University, 3-4-1, Okubo, Shinjuku, Tokyo 169-8555, Japan. E-mail: takenobu@waseda.jp

† Electronic Supplementary Information (ESI) available: <sup>1</sup>H, <sup>13</sup>C NMR and MALDI-TOF mass spectra, cyclic voltammograms, fluorescence spectra, fluorescence titration spectra, <sup>1</sup>H NMR titration, femtosecond laser-induced transient absorption spectral measurement data, and DFT data. See DOI: 10.1039/b000000x/

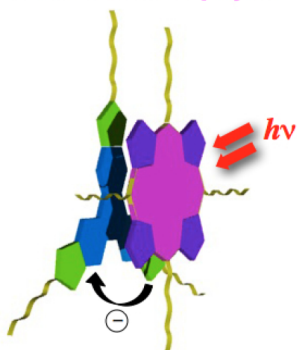
- 1 (a) S. Kirner, M. Sekita and D. M. Guldi, *Adv. Mater.*, 2014, **26**, 1482-1493; (b) J. Malig, N. Jux and D. M. Guldi, *Acc.*

- Chem. Res.*, 2013, **46**, 53-64; (c) G. Bottari, G. De la Torre, D. M. Guldi, T. Torres, *Chem. Rev.*, 2010, **110**, 6768-6816.
- 2 (a) D. Gust, T. A. Moore and A. L. Moore, *Acc. Chem. Res.*, 2009, **42**, 1890-1898; (c) M. R. Wasielewski, *Acc. Chem. Res.*, 2009, **42**, 1910-1921; (d) J. Frey, G. Kodis, S. D. Straight, T. A. Moore, A. L. Moore and D. Gust, *J. Phys. Chem. A*, 2013, **117**, 607-615.
- 3 (a) S. Fukuzumi, K. Ohkubo and T. Suenobu, *Acc. Chem. Res.*, 2014, **47**, 1455-1464; (b) S. Fukuzumi, *Phys. Chem. Chem. Phys.*, 2008, **10**, 2283-2297; (c) K. Ohkubo and S. Fukuzumi, *Bull. Chem. Soc. Jpn.*, 2009, **82**, 303-315; (d) S. Fukuzumi, *Bull. Chem. Soc. Jpn.*, 2006, **79**, 177-195; (e) S. Fukuzumi, *Org. Biomol. Chem.*, 2003, **1**, 609-620.
- 4 (a) Q. Yan, Z. Luo, K. Cai, Y. Ma and D. Zhao, *Chem. Soc. Rev.*, 2014, **43**, 4199-4221; (b) P. D. Frischmann, K. Mahata and F. Würthner, *Chem. Soc. Rev.*, 2013, **42**, 1847-1870; (c) Y. K. Kang, P. M. Iovine and M. J. Therien, *Coord. Chem. Rev.*, 2011, **255**, 804-824; (d) B. Albinsson and J. Mårtensson, *J. Photochem. Photobiol. C: Photochem. Rev.*, 2008, **9**, 138-155.
- 5 (a) M. E. El-Khouly, S. Fukuzumi, and F. D'Souza, *ChemPhysChem* 2014, **15**, 30-47; (b) F. D'Souza and O. Ito, *Chem. Soc. Rev.*, 2012, **41**, 86-96; (c) S. Fukuzumi, K. Ohkubo, F. D'Souza and J. L. Sessler, *Chem. Commun.*, 2012, **48**, 9801-9815; (d) F. D'Souza and O. Ito, *Chem. Commun.*, 2009, 4913-4928; (e) R. Chitta and F. D'Souza, *J. Mater. Chem.*, 2008, **18**, 1440-1471.
- 6 (a) M. Natali, S. Campagna and F. Scandola, *Chem. Soc. Rev.*, 2014, **43**, 4005-4018; (b) A. Arrigo, A. Santoro, M. T. Indelli, M. Natali, F. Scandola and S. Campagna, *Phys. Chem. Chem. Phys.*, 2014, **16**, 818-826; (c) D. Hanss, M. E. Walther and O. S. Wenger, *Coord. Chem. Rev.*, 2010, **254**, 2584-2592.
- 7 (a) D. M. Guldi and R. D. Costa, *J. Phys. Chem. Lett.*, 2013, **4**, 1489-1501; (b) K. Tambara and G. D. Santos, *Annu. Rep. Prog. Chem., Sect. B: Org. Chem.*, 2012, **108**, 186-201.
- 8 G. Bottari, O. Trukhina, M. Ince and T. Torres, *Coord. Chem. Rev.*, 2012, **256**, 2453-2477.
- 9 (a) S. Fukuzumi and K. Ohkubo, *Dalton Trans.*, 2013, **42**, 15846-15858; (b) S. Fukuzumi and K. Ohkubo, *J. Mater. Chem.*, 2012, **22**, 4575-4587; (b) S. Fukuzumi, T. Honda and T. Kojima, *Coord. Chem. Rev.*, 2012, **256**, 2488-2502.
- 10 (a) J. L. Sessler, B. Wang and A. Harriman, *J. Am. Chem. Soc.*, 1993, **115**, 10418-10419; (b) F. Wessendorf, J.-F. Gnichwitz, G. H. Sarova, K. Hager, U. Hartnagel, D. M. Guldi, A. Hirsch, *J. Am. Chem. Soc.* 2007, **129**, 16057-16071; (c) H. Kar and S. Ghosh, *Chem. Commun.*, 2014, **50**, 1064-1066; (d) S. Verma, A. Ghosh, A. Das and H. N. Ghosh, *Chem. Eur. J.*, 2011, **17**, 3458-3464; (e) S. Murphy, L. Huang and P. V. Kamat, *J. Phys. Chem. C*, 2011, **115**, 22761-22769.
- 11 (a) M. Gallego, J. Calbo, J. Aragó, R. M. Krick Calderon, F. H. Liquido, T. Iwamoto, A. K. Greene, E. A. Jackson, E. M. Pérez, E. Ortí, D. M. Guldi, L. T. Scott and N. Martín, *Angew. Chem., Int. Ed.*, 2014, **53**, 2170-2175; (b) K. S. Suslick and R. A. Watson, *New J. Chem.*, 1992, **16**, 633-642; (c) I. Duchemin and X. Blase, *Phys. Rev. B*, 2013, **87**, 245412.
- 12 (a) N. L. Bill, M. Ishida, Y. Kawashima, K. Ohkubo, Y. M. Sung, V. M. Lynch, J. M. Lim, D. Kim, J. L. Sessler and S. Fukuzumi, *Chem. Sci.*, 2014, **5**, 3888-3896; (b) N. L. Bill, M. Ishida, S. Bähring, J. M. Lim, S. Lee, C. M. Davis, V. M. Lynch, K. A. Nielsen, J. O. Jeppesen, K. Ohkubo, S. Fukuzumi, D. Kim and J. L. Sessler, *J. Am. Chem. Soc.*, 2013, **135**, 10852-10862; (c) C. M. Davis, Y. Kawashima, K. Ohkubo, J. M. Lim, D. Kim, S. Fukuzumi and J. L. Sessler, *J. Phys. Chem. C*, 2014, **118**, 13503-13513.
- 13 (a) P. Li, S. Amirjalayer, F. Hartl, M. Lutz, B. de Bruin, R. Becker, S. Woutersen, J. N. H. Reek, *Inorg. Chem.*, 2014, **53**, 5373-5383; (b) P. K. Poddutoori, N. Zarrabi, A. G. Moiseev, R. Gumbau-Brisa, S. Vassiliev, A. van der Est, *Chem.-Eur. J.*, 2013, **19**, 3148-3161; (c) E. Iengo, G. Dan Pantosx, J. K. M. Sanders, M. Orlandi, C. Chiorboli, S. Fracasso and F. Scandola, *Chem. Sci.*, 2011, **2**, 676-685.
- 14 (a) T. Kamimura, K. Ohkubo, Y. Kawashima, H. Nobukuni, Y. Naruta, F. Tani and S. Fukuzumi, *Chem. Sci.*, 2013, **4**, 1451-1461; (b) H. Nobukuni, Y. Shimazaki, H. Uno, Y. Naruta, K. Ohkubo, T. Kojima, S. Fukuzumi, S. Seki, H. Sakai, T. Hasobe and F. Tani, *Chem.-Eur. J.*, 2010, **16**, 11611-11623.
- 15 (a) Y. Kawashima, K. Ohkubo, K. Mase and S. Fukuzumi, *J. Phys. Chem. C*, 2013, **117**, 21166-21177; (b) K. Ohkubo, Y. Kawashima and S. Fukuzumi, *Chem. Commun.*, 2012, **48**, 4314-4316; (c) S. Fukuzumi, K. Ohkubo, Y. Kawashima, D. S. Kim, J. S. Park, A. Jana, V. M. Lynch, D. Kim, J. L. Sessler, *J. Am. Chem. Soc.*, 2011, **133**, 15938-15941.
- 16 (a) S. Fukuzumi, T. Honda, T. Kojima, *Coord. Chem. Rev.*, 2012, **256**, 2488-2502; (b) M. Kanematsu, P. Naumov, T. Kojima and S. Fukuzumi, *Chem.-Eur. J.*, 2011, **17**, 12372-12384; (c) T. Honda, T. Nakanishi, K. Ohkubo, T. Kojima and S. Fukuzumi, *J. Am. Chem. Soc.*, 2010, **132**, 10155-10163; (d) T. Kojima, T. Honda, K. Ohkubo, M. Shiro, T. Kusakawa, T. Fukuda, N. Kobayashi and S. Fukuzumi, *Angew. Chem., Int. Ed.*, 2008, **47**, 6712-6716.
- 17 (a) F. D'Souza, A. N. Amin, M. E. El-Khouly, N. K. Subbaiyan, M. E. Zandler and S. Fukuzumi, *J. Am. Chem. Soc.*, 2012, **134**, 654-664; (b) S. Fukuzumi, K. Saito, K. Ohkubo, T. Khoury, Y. Kashiwagi, M. A. Absalom, S. Gadde, F. D'Souza, Y. Araki, O. Ito and M. J. Crossley, *Chem. Commun.*, 2011, **47**, 7980-7982; (c) M. E. El-Khouly, D. K. Ju, K.-Y. Kay, F. D'Souza and S. Fukuzumi, *Chem.-Eur. J.*, 2010, **16**, 6193-6202; (d) A. Takai, M. Chkounda, A. Eggenspieler, C. P. Gros, M. Lachkar, J.-M. Barbe and S. Fukuzumi, *J. Am. Chem. Soc.*, 2010, **132**, 4477-4489; (e) F. D'Souza, E. Maligaspe, K. Ohkubo, M. E. Zandler, N. K. Subbaiyan and S. Fukuzumi, *J. Am. Chem. Soc.*, 2009, **131**, 8787-8797; (f) F. D'Souza, N. K. Subbaiyan, Y. Xie, J. P. Hill, K. Ariga, K. Ohkubo and S. Fukuzumi, *J. Am. Chem. Soc.*, 2009, **131**, 16138-16146; (g) V. Bandi, M. E. El-Khouly, K. Ohkubo, V. N. Nesterov, M. E. Zandler, S. Fukuzumi and F. D'Souza, *J. Phys. Chem. C*, 2014, **118**, 2321-2332; (h) C. B. K. C, S. K. Das, K. Ohkubo, S. Fukuzumi and F. D'Souza, *Chem. Commun.*, 2012, **48**, 11859-11861.
- 18 (a) S. Fukuzumi and T. Kojima, *J. Mater. Chem.*, 2008, **18**, 1427-1439; (b) T. Kojima, T. Nakanishi, T. Honda and S. Fukuzumi, *J. Porphyrins Phthalocyanines*, 2009, **13**, 14-21; (c) S. Fukuzumi, T. Honda, K. Ohkubo and T. Kojima, *Dalton Trans.*, 2009, 3880-3889; (d) T. Kojima, K. Hanabusa, K. Ohkubo, M. Shiro, S. Fukuzumi, *Chem.-Eur. J.*, 2010, **16**, 3646-3655; (e) T. Honda, T. Nakanishi, K. Ohkubo, T. Kojima and S. Fukuzumi, *J. Phys. Chem. C*, 2010, **114**, 14920-14299.
- 19 (a) P. Mondal, A. Chaudhary and S. P. Rath, *Dalton Trans.*, 2013, **42**, 12381-12394; (b) A. Chaudhary and S. P. Rath, *Chem.-Eur. J.*, 2012, **18**, 7404-7417; (c) S. Fukuzumi, I. Amasaki, K. Ohkubo, C. P. Gros, R. Guillard, J.-M. Barbe, *RSC Adv.*, 2012, **2**, 3741-3747; (d) S.

- S. Gayathri, M. Wielopolski, E. M. Pérez, G. Fernández, L. Sánchez, R. Viruela, E. Ortí, D. M. Guldi, N. Martín, *Angew. Chem., Int. Ed.*, 2009, **48**, 815-819; (e) M. Tanaka, K. Ohkubo, C. P. Gros, R. Guilard and S. Fukuzumi, *J. Am. Chem. Soc.*, 2006, **128**, 14625-14633.
- 20 (a) P. D. Harvey, C. Stern and R. Guilard, in *Handbook of Porphyrin Science with Applications to Chemistry, Physics, Materials Science, Engineering, Biology and Medicine*, ed. K. M., Kadish, K. M. Smith and R. Guilard, World Scientific Publishing: Singapore, 2011, vol. 11, p. 1-177; (b) M. K. Panda, K. Ladomenou and A. G. Coutsolelos, *Coord. Chem. Rev.*, 2012, **256**, 2601-2627; (c) J. Yang, M.-C. Yoon, H. Yoo, P. Kim and D. Kim, *Chem. Soc. Rev.*, 2012, **41**, 4808-4826; (d) V. K. Praveen, C. Ranjith, E. Bandini, A. Ajayaghosh, N. Armaroli, *Chem. Soc. Rev.*, 2014, **43**, 4222-4242.
- 21 (a) N. Aratani, D. Kim and A. Osuka, *Acc. Chem. Res.*, 2009, **42**, 1922-1934; (b) A. Uetomo, M. Kozaki, S. Suzuki, K.-i. Yamanaka, O. Ito, K. Okada, *J. Am. Chem. Soc.*, 2011, **133**, 13276-13279; (c) J.-M. Camus, S. M. Aly, D. Fortin, R. Guilard and P. D. Harvey, *Inorg. Chem.*, 2013, **52**, 8360-8368.
- 22 (a) M. Beyler, L. Flamigni, V. Heitz, J.-P. Sauvage and B. Ventura, *Photochem. Photobiol.*, 2014, **90**, 275-286; (b) A. Satake and Y. Kobuke, *Tetrahedron*, 2005, **61**, 13-41; (c) F. Hajjaj, Z. S. Yoon, M.-C. Yoon, J. Park, A. Satake, D. Kim and Y. Kobuke, *J. Am. Chem. Soc.*, 2006, **128**, 4612-4623.
- 23 D. Adam, P. Schuhmacher, J. Simmerer, L. Haeussling, K. Siemensmeyer, K. H. Etzbach, H. Ringsdorf and D. Haarer, *Nature*, 1994, **371**, 141-143.
- 24 Y. Wang, C. Zhang, H. Wu and J. Pu, *J. Mater. Chem. C*, 2014, **2**, 1667-1674.
- 25 (a) K. S. Mali, M. G. Schwab, X. Feng, K. Müllen and S. De Feyter, *Phys. Chem. Chem. Phys.*, 2013, **15**, 12495-12503; (b) F. Hu, Y. Gong, X. Zhang, J. Xue, B. Liu, T. Lu, K. Deng, W. Duan, Q. Zeng and C. Wang, *Nanoscale*, 2014, **6**, 4243-4249.
- 26 R. Nasielski-Hinkens, M. Benedek-Vamos, D. Maetens and J. Nasielski, *J. Organomet. Chem.*, 1981, **217**, 179-182.
- 27 R. Juárez, M. M. Oliva, M. Ramos, J. L. Segura, C. Alemán, F. Rodríguez-Ropero, D. Curcó, F. Montilla, V. Coropceanu, J. L. Brédas, Y. Qi, A. Kahn, M. C. Ruiz Delgado, J. Casado and J. T. López Navarre, *Chem.–Eur. J.*, 2011, **17**, 10312-10322.
- 28 G. Aragay, A. Frontera, V. Lloveras, J. Vidal-Gancedo and P. Ballester, *J. Am. Chem. Soc.*, 2013, **135**, 2620-2627.
- 29 T. Chiba, Y.-J. Pu, R. Miyazaki, K.-i. Nakayama, H. Sasabe and J. Kido, *Org. Electronics*, 2011, **12**, 710-715.
- 30 K. Pieterse, P. A. van Hal, R. Kleppinger, J. A. J. M. Vekemans, R. A. J. Janssen and E. W. Meijer, *Chem. Mater.*, 2001, **13**, 2675-2679.
- 31 D. Dubois, K. M. Kadish, S. Flanagan, R. E. Hauffer, L. P. F. Chibante and L. Wilson, *J. Am. Chem. Soc.*, 1991, **113**, 4364-4366.
- 32 L. M. Klivansky, D. Hanifi, G. Koshkaryan, D. R. Holycross, E. K. Gorski, Q. Wu, M. Chai and Y. Liu, *Chem. Sci.*, 2012, **3**, 2009-2014.
- 33 K. Kanakarajan and A. W. Czarnik, *J. Org. Chem.*, 1986, **51**, 5241-5243.
- 34 K. Kanakarajan and A. W. Czarnik, *J. Heterocyclic Chem.*, 1988, **25**, 1869-1872.
- 35 M. J. Crossley, P. Thordarson, J. P. Bannerman and P. J. Maynard, *J. Porphyrins Phthalocyanines*, 1998, **2**, 511-516.
- 36 Z.-G. Tao, X. Zhao, X.-K. Jiang and Z.-T. Li, *Tetrahedron Lett.*, 2012, **53**, 1840-1842.
- 37 S. Hirayama, H. Sakai, Y. Araki, M. Tanaka, M. Imakawa, T. Wada, T. Takenobu and T. Hasobe, *Chem.–Eur. J.*, 2014, **20**, 9081-9093.
- 38 K. Ida, H. Sakai, K. Ohkubo, Y. Araki, T. Wada, T. Sakanoue, T. Takenobu, S. Fukuzumi and T. Hasobe, *J. Phys. Chem. C*, 2014, **118**, 7710-7720.
- 39 (a) I. B. Berlman, In *Handbook of Fluorescence Spectra of Aromatic Molecules Second Ed.*; Academic Press, New York, 1971, p 473; (b) in *Handbook of Photochemistry*, eds. M. Motalti, A. Credi, L. Prodi and M. T. Gandolfi, CRC Press, Boca Raton, 3rd edn., 2006, pp. 83-157.
- 40 O. Reiser, B. Koenig, K. Meerholz, J. Heinze, T. Wellauer, F. Gerson, R. Frim, M. Rabinovitz and A. de Meijere, *J. Am. Chem. Soc.*, 1993, **115**, 3511-3518.
- 41 S. L. Mattes and S. Farid, In *Organic Photochemistry*, ed. A. Padwa, Marcel Dekker, New York, 1983, Vol. 6, p 233.
- 42 J. Yin, H. Qu, K. Zhang, J. Luo, X. Zhang, C. Chi and J. Wu, *Org. Lett.*, 2009, **11**, 3028-3031.
- 43 L. Tan-Sien-Hee and A. Kirsch-De Mesmaeker, *J. Chem. Soc., Dalton Trans.*, 1994, 3651-3658.
- 44 Z. Gasyna, W. R. Browett and M. Stillman, *J. Inorg. Chem.*, 1985, **24**, 2440-2447.
- 45 S. Fukuzumi, T. Suenobu, M. Patz, T. Hirasaka, S. Itoh, M. Fujitsuka and O. Ito, *J. Am. Chem. Soc.*, 1998, **120**, 8060-8068.
- 46 S. Fukuzumi, K. Ohkubo, Y. Kawashima, D. S. Kim, J. S. Park, A. Jana, V. M. Lynch, D. Kim and J. L. Sessler, *J. Am. Chem. Soc.*, 2011, **133**, 15938-15941.
- 47 No additional emission band was observed even though we excited the higher energy band (i.e., Soret band at ca. 420 nm).
- 48 P. V. Bernhardt and E. Hayes, *J. Inorg. Chem.*, 2003, **42**, 1371-1377.
- 49 The stabilization energy ( $E_{\text{stab}}$ ) of porphyrin and HAT-TIm was estimated from the following equation:  $E_{\text{stab}} = E_{\text{DA}} - (E_{\text{D}} + E_{\text{A}})$ , where  $E_{\text{DA}}$  is the total energy of the D-A assembly,  $E_{\text{D}}$  and  $E_{\text{A}}$  are the total energies of the each component. The calculated energies at the B3LYP/6-31(d) level of theory are summarized in Table S20 in ESI. For example, the difference of stabilization energies between ZnP-C<sub>3</sub>HAT-TIm and ZnP-C<sub>6</sub>HAT-TIm was 0.06 kcal mol<sup>-1</sup>. Similarly, the difference was also estimated to be 0.13 kcal mol<sup>-1</sup> in the case of H<sub>2</sub>P-C<sub>3</sub>HAT-TIm and H<sub>2</sub>P-C<sub>12</sub>HAT-TIm. These results indicate that hydrophobic interactions form between alkyl chains can be neglected. See the following reference paper: P. R. Bangal, *J. Phys. Chem. A*, 2007, **111**, 5536-5543.
- 50 Dispersion-corrected calculation methods (e.g. WB97XD) were inconsistent with the absorption of CT  $\pi$ -complex (Fig. 6A).
- 51 T. Hasobe, H. Imahori, P. V. Kamat, T. K. Ahn, S. K. Kim, D. Kim, A. Fujimoto, T. Hirakawa and S. Fukuzumi, *J. Am. Chem. Soc.*, 2005, **127**, 1216-1228.
- 52 J. L. Sessler, E. Karnas, S. K. Kim, Z. Ou, M. Zhang, K. M. Kadish, K. Ohkubo and S. Fukuzumi, *J. Am. Chem. Soc.*, 2008, **130**, 15256-15257.
- 53 K. Ohkubo, K. Mase, E. Karnas, J. L. Sessler and S. Fukuzumi, *J. Phys. Chem. C*, 2014, **118**, 19436-18444.
- 54 T. Honda, T. Nakanishi, K. Ohkubo, T. Kojima and S. Fukuzumi, *J. Am. Chem. Soc.*, 2010, **132**, 10155-10163.

- 55 T. Hasobe, M. G. Rabbani, A. S. D. Sandanayaka, H. Sakai and T. Murakami, *Chem. Commun.*, 2010, **46**, 889-891.
- 56 *Gaussian 09, revision A.02*, Gaussian, Inc., Wallingford, CT, 2009.
- 57 R., II Dennington, T. Keith, J. Millam, K. Eppinnett, W. L. Hovell and R. Gilliland, *GaussView*, Semichem, Shawnee Mission, KS, 2003.

## Table of Contents

**Supramolecular  $\pi$ -Complex  
in HAT-TIm/Porphyrin****Ultrafast  
Electron Transfer**

We have successfully observed ultrafast photoinduced electron transfer in face-to-face charge-transfer  $\pi$ -complexes of planar porphyrins and hexaazatriphenylene derivatives.